Solar Energy Materials & Solar Cells 94 (2010) 1816–1821

Contents lists available at ScienceDirect

Solar Energy Materials & Solar Cells

journal homepage: www.elsevier.com/locate/solmat

A new approach to the solvent system for inkjet-printed P3HT:PCBM solar cells and its use in devices with printed passive and active layers

Alexander Lange [a,*], Michael Wegener [a], Christine Boeffel [a], Bert Fischer [a], Armin Wedel [a], Dieter Neher [b]

[a] Fraunhofer Institute for Applied Polymer Research, Geiselbergstrasse 69, 14476 Potsdam, Germany
[b] University of Potsdam, Institute of Physics and Astronomy, Karl-Liebknecht-Strasse 24-25, 14476 Potsdam, Germany

ARTICLE INFO

Article history:
Received 8 April 2010
Received in revised form
28 May 2010
Accepted 28 May 2010
Available online 15 June 2010

Keywords:
Inkjet
P3HT
PCBM
OPV
Organic photovoltaics

ABSTRACT

Inkjet-printing is a suitable method to generate patterned structures from solvents containing active components. However, the process of inkjet-printing imposes severe limitations on the properties of the inkjet ink. This paper presents a new approach to solvent systems suitable for inkjet-printing common organic solar cell materials, poly(3-hexylthiophene) and 1-(3-methoxycarbonyl)propyl-1-phenyl[6,6]C_{61} as active layers in solar cells. Typically, low boiling point chlorinated solvents are used to dissolve P3HT and PCBM because both components are well soluble in these materials. During inkjet-printing, nozzle clogging due to evaporation of the ink in the inkjet print head is reduced when a high boiling point solvent is incorporated. Solar cells with active layers that were printed from an ink with a solvent system of chlorobenzene and trichlorobenzene showed power conversion efficiencies of 2.4% when active layer was dried at 130 °C. This compares to 2.6% for spin-coated solar cells from the same materials. In addition, devices with printed passive and printed active layers were prepared and power conversion efficiencies of 1.5% were achieved.

1. Introduction

Organic electronics offer the potential for light-weight and large-scale electronic and optoelectronic devices, e.g. organic field-effect transistors (OFETs), organic light emitting diodes (OLEDs) and organic photovoltaics (OPVs). Among these different categories, polymer based solar cells have received considerable attention during the past several years and a wide range of polymeric materials accessible via organic chemistry have been employed to convert sunlight into electricity with high efficiency [1–3]. Today, several techniques are being used to deposit the active polymer layers onto stiff or flexible substrates, including spin-coating, doctor blading, slot die coating and printing [1]. Also, the deposition of various layers of a polymer solar cell with low cost roll-to-roll technology on flexible substrates with large device areas has been demonstrated [4,5]. Furthermore, polymer solar cells have also undergone round robin studies and field testing, which demonstrate that this technology is useful and well underway to further commercial development and additional integration into the marketplace [6,7]. In contrast with semi-industrial scale studies, other works have focused on smaller devices, where different interlayers were examined for their impact on performance in addition to the influence of additives, thermal and solvent annealing on the efficiency as shown in a recent review [8]. Specifically, devices with inverted structures have demonstrated similar performances to traditional cells, which shows the versatility and flexibility of this technology [8]. It can be concluded that the first step has been taken in commercialization of polymer solar cells and that a positive future awaits.

Among the various methods for depositing the active materials from solution, inkjet-printing is mostly suited to generate patterned structures. Despite the somewhat slower speed of inkjet-printing with respect to other printing techniques, this technology theoretically could be incorporated into a roll-to-roll process. However, as pointed out in the literature this has not yet been accomplished [1]. The deposition of layers by ejection of droplets from a printing head during inkjet-printing imposes severe restrictions on the properties of the solution containing the active materials. Therefore, understanding how to properly formulate inkjet inks for organic electronic devices is necessary for future inkjet applications.

In this work, the photo-active materials poly(3-hexylthiophene) (P3HT) and 1-(3-methoxycarbonyl)propyl-1-phenyl [6,6]C_{61} (PCBM) were inkjet-printed and solar cells with printed layers are compared to solar cells with spin-coated layers. In contrast with inkjet-printing, spin-coating relies on the spreading of the solvent due to a centrifugal force. Here, various parameters such as concentration of the solution, spinning speed and spinning time can be independently varied to find the optimum conditions for a given solvent. The goal of this work was to understand how inkjet-printing influences a photo-active

* Corresponding author. Tel.: +49 331 568 1913; fax: +49 331 568 3910.
E-mail addresses: alange@iap.fhg.de, alange@iap.fraunhofer.de (A. Lange).

0927-0248/$ - see front matter © 2010 Elsevier B.V. All rights reserved.
doi:10.1016/j.solmat.2010.05.054

system and what requirements are needed to successfully print this system.

Bulk heterojunction organic solar cells with active layers made from P3HT and PCBM have demonstrated power conversion efficiencies (η_{PCE}) of up to 5% [9]. In addition, organic solar cells based on other materials such as copolymers of poly(carbazole) and poly(benzothiadiazole) (PCDTBT) and [6,6]-phenyl C70-butyric acid methyl ester ($PC_{70}BM$) have been shown to reach internal quantum efficiencies close to 100% [10]. These two examples demonstrate that organic photovoltaic (OPV) devices are able to effectively convert solar light into electricity. Most organic solar cells have been produced with spin-coating [9,10]. Here, chlorinated solvents are generally used because P3HT and PCBM are well soluble in these solvents. Optimized solvent mixtures and preparation conditions have yielded average efficiencies up to 4% [3,11]. Unfortunately, conditions for obtaining optimum results for spin-coated solar cells cannot be directly applied to layers generated by inkjet-printing. One major difference is that inkjet inks need a high boiling point to prevent print head nozzle clogging as well as the coffee stain effect, which has been well documented [12,13]. At the same time, poor P3HT:PCBM solubility in the high boiling point component may occur, resulting in rather different active layer morphologies.

Inkjet-printing of P3HT:PCBM has been successfully demonstrated with inks based on dichlorobenzene/mesitylene and tetralin where the η_{PCE} reached 2.90% and 1.29%, respectively [14]. An even higher efficiency of 3.50% was achieved with a dichlorobenzene/mesitylene system when the degree of P3HT regioregularity was optimized for the inkjet-printing process [15,16]. When an inkjet solvent system based on chlorobenzene/tetralin is used, a η_{PCE} of 1.40% was reported [17]. As stated earlier, the solubility of P3HT:PCBM in high boiling solvents such as mesitylene and tetralin may not be good relative to the solubility of P3HT:PCBM in chlorinated solvents. Therefore, optimizing the solubility of P3HT:PCBM in all constituents of the solvent system should be considered when designing an inkjet ink.

Here, we demonstrate that the combination of chlorobenzene and trichlorobenzene is a highly suitable solvent system for the preparation of efficient P3HT:PCBM solar cells via inkjet-printing. In fact, the η_{PCE} of solar cells with printed active layers was 2.4% when optimized drying conditions were used, which is similar to the efficiency achieved for spin-coated devices in our laboratory. This is explained by the rather good solubility of P3HT in trichlorobenzene. When this ink was inkjet-printed onto inkjet-printed passive layers, a η_{PCE} of 1.5% was obtained. To our knowledge, this is currently the highest reported performance for a solar cell with an inkjet-printed passive and an inkjet-printed active layer.

2. Experimental details

Before spin-coating or inkjet-printing, patterned ITO substrates (Optrex GmbH, 20 /□) were cleaned in a 2 vol% solution of Deconex in DI water for 15 min in an ultrasonic bath. After drying with nitrogen, the substrates were treated with O_2 plasma for 3 min (120 W).The passive layer was either spin-coated from a commercial PEDOT:PSS dispersion (AI4083 from H.C. Stark) at 2500 RPM in air or it was inkjet-printed from diluted Plextronics Plexcore (25 wt% isopropanol and 25 wt% ethylene glycol). The passive layers were roughly 30 nm thick after spin coating and 110 nm thick after inkjet-printing. All passive layers were dried at 180 °C for 35 min in an inert atmosphere. For spin-coating of the active layer, a 1:1 solution of P3HT:PCBM (both from American Dye Source) in chlorobenzene was used with a concentration of 1.4 wt% P3HT. The number average molecular weight (M_n) of the P3HT was estimated with gel permeation chromatography against polystyrene standards to be 23,000 g/mol. Spin-coating of the active layer was done at 1500 RPM in an inert atmosphere, which generated 110 nm thick films. Pre-annealing was performed at 100 °C for 30 min. Inkjet-printing of the passive and active layer was done in an inert atmosphere with a Pixdro LP150 printer. The P3HT:PCBM ink for the active layer consisted of a 55 wt% chlorobenzene and 45 wt% trichlorobenzene mixture with 0.30 wt% concentration of P3HT in a 1:1 wt/wt P3HT:PCBM ratio. This P3HT concentration gave a printed film thickness of approximately 180 nm. Immediately after printing, the films were dried at 100, 130 or 160 °C until the printed active layer underwent the liquid/solid transition followed by pre-annealing at 100 or 140 °C for 30 min. The drying process took no longer than ~30 s at 100 °C and ~5 s at 160 °C. Inkjet-printed passive and active layer edge effects were not considered because the dimensions of the printed films were greater than those of the solar cell active area. Thus, any edge effects occurred outside the active area and they were ignored. The aluminium cathode was evaporated at 10^{-6} mbar with a resulting thickness of 120 nm, giving a device active area of 0.16 cm^2. After evaporation, post-annealing was performed at 150 °C for 10 min for all of the devices. The solar cells were measured at 100 mW/cm^2 with a Steuerangel solar simulator (AM 1.5) in conjunction with a Keithley 2400 source meter. The surface topography was measured with atomic force microscopy (AFM) in contact modes with a Nanosurf AFM. UV–vis spectra were recorded with a Perkin Elmer Lambda 950 spectrometer and all UV–vis solutions had concentrations of 0.01 wt%. Before measuring, the UV–vis solutions were heated at 70 °C, mixed overnight and heated again approximately for 15 min before recording the UV–vis spectra. To determine the incident photon to converted electron efficiency (*IPCE*), the wavelength was set by an Oriel Cornerstone 260 monochromator in conjunction with an Oriel 150 W Xe-lamp. A calibrated silicon diode was used to determine the spectral intensity of the light source where the current was measured with a Harvard Research lock-in amplifier.

3. Results and discussion

3.1. Absorbance properties of P3HT:PCBM

In order to test the suitability of potential solvents for inkjet-printing, UV–vis spectroscopy was performed on P3HT:PCBM in solution. The solvents selected for examination were chlorobenzene, trichlorobenzene and mesitylene. Chlorobenzene was selected because chlorinated solvents are typically good solvents for P3HT while trichlorobenzene was chosen because it has a boiling point of over 200 °C [18]. Due to its occurrence in the inkjet literature involving the formation of P3HT:PCBM films, mesitylene was also selected. Furthermore, the absorption properties of a mixture of chlorobenzene and trichlorobenzene (55 wt% chlorobenzene, 45 wt% trichlorobenzene) with P3HT:PCBM were studied. In order to directly compare the solubility properties of UV–vis solutions under examination and inkjet inks, the absorbance properties of P3HT:PCBM solutions with concentrations matching inkjet inks (0.30 wt%) should be measured. For this report, concentrations of 0.01 wt% were used because it was found that more concentrated solutions (0.04 wt%) resulted in signal saturation. Fig. 1 shows the absolute absorbance spectra of the chlorobenzene (a), trichlorobenzene (b), mesitylene (c) and the chloro-/trichlorobenzene solutions.

Based on the chemical nature of a respective solvent and its interaction with P3HT and PCBM, different characteristics can be seen in the UV–vis spectrum. All four of the spectra in Fig. 1 show

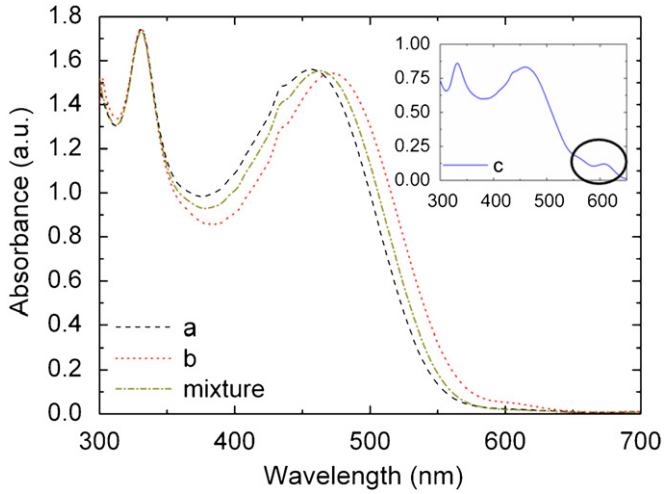

Fig. 1. Absolute absorbance versus wavelength for 1:1 (wt/wt) P3HT:PCBM in chlorobenzene (a), trichlorobenzene (b), mesitylene (c) and in a mixture of chlorobenzene and trichlorobenzene representing an inkjet ink.

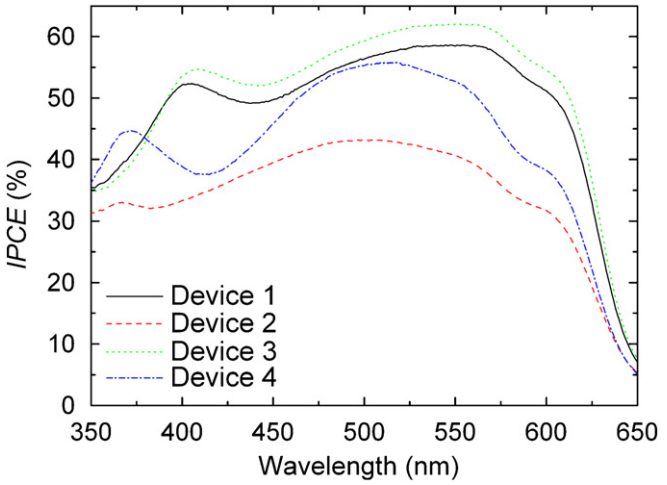

Fig. 2. *IPCE* efficiency versus wavelength for solar cells with printed P3HT:PCBM layers that were dried at 100 °C and pre-annealed at 100 °C (device 1), dried at 100 °C and pre-annealed at 140 °C (device 2), dried at 130 °C and pre-annealed at 100 °C (device 3) and dried at 160 °C and pre-annealed at 100 °C (device 4).

the characteristic PCBM and P3HT peaks at ~320 and ~460 nm, respectively. It has been shown that in P3HT:PCBM films, PCBM and P3HT absorb at 320 and 550 nm, respectively [11,19]. Furthermore, the UV–vis spectra of P3HT:PCBM solutions typically illustrate the characteristic P3HT peak at ~460 nm [20]. The blue-shift in the P3HT peak for P3HT:PCBM solutions versus films is due to a change in the polymer's conjugation length when dissolved in a solvent. On the other hand, a small red-shift is seen in Fig. 1 as the solvent is changed from chloro- to trichlorobenzene. This shift could be caused by a chemical interaction of trichlorobenzene with P3HT resulting in conjugation length changes or due to the different polarities of the solvents. In contrast with the other three solutions, the mesitylene solution displayed in the inset of Fig. 1 shows aggregation. This is supported by the low energy bands at 560 and 605 nm, which are characteristic of aggregated chains [20].

In addition to the spectra of P3HT:PCBM with chloro- or trichlorobenzene, the chloro-/trichlorobenzene mixture spectrum does not show any aggregation bands at 560 or 605 nm. The solvent mixture spectrum resembles a combination of the chloro- and trichlorobenzene solution spectra, where the maximum P3HT absorbance occurs between those of the two respective solutions. The absence of aggregation bands shows that the chloro-/trichlorobenzene solvent mixture is beneficial for inkjet-printing because it offers good P3HT solubility and a high boiling point.

3.2. Characterization of solar cells with inkjet-printed and spin-coated organic layers

Because printed films are still in a fluid state after printing, they were immediately heated to dry the layer. For the printed active layers considered in this report, the drying step was no longer than 30 s. It is likely that the printed films did not reach the set point of the hot plate due to the short drying time. Instead, a higher drying temperature resulted in a faster rate of drying where the liquid to solid transition of the P3HT:PCBM film occurred more rapidly. The influence of drying conditions on the incident photon to converted electron (*IPCE*) efficiency is shown in Fig. 2, which illustrates the spectral responses of solar cells with active layers that were dried at selected temperatures. For example, solar cell active layers were dried at 100 °C and pre-annealed at 100 °C (device 1), dried at 100 °C and pre-annealed at 140 °C (device 2), dried at 130 °C and pre-annealed at 100 °C (device 3) and dried at 160 °C and pre-annealed at 100 °C (device 4). In addition to drying printed films and pre-annealing, all of the devices discussed in this report were post-annealed at 150 °C for 10 min. Here, pre-annealing occurred before evaporation of the cathode and post-annealing occurred after evaporation of the cathode.

Solar cells with printed active layers that were dried at 100 (device 1) and 130 °C (device 3) showed peak *IPCE* values of approximately 58% and 62%, respectively, as shown in Fig. 2. This compares to roughly 54% for active layers that were dried at 160 °C (device 4). Pre-annealing at 140 °C (device 2) reduced the peak *IPCE* to less than 40%, which we attribute to crystallization of PCBM that was visible with the eye after the thermal treatment. It has been shown that the preparation and annealing conditions influence the *IPCE* efficiency of P3HT:PCBM solar cells, where a range of values from 58% to 87% was reported [3]. The values generated for the solar cells here correspond well to the *IPCE* range stated in the literature. The differences in Fig. 2 for the three films that were pre-annealed at 100 °C are proposed to be due to organization of P3HT at different drying temperatures. This is supported by absorption over a wider range of wavelengths in Fig. 2 for devices with layers that were dried at 100 and 130 °C versus 160 °C. The importance of drying time on performance of solar cells with spin-coated P3HT:PCBM active layers that were processed under different conditions has been previously demonstrated [21,22]. Furthermore, drying the active layer at 160 °C can negatively influence thin film morphology because this drying temperature resulted in a device with a η_{PCE} of 1.2%. This compares to an average value of ~2.3% for active layers that were dried at 100 and 130 °C.

Similar performance between solar cells with printed active layers from the chloro-/trichlorobenzene solvent mixture and solar cells prepared with well-established preparation methods like spin-coating was an important aim of this work. Fig. 3 shows a plot of current density versus voltage measured under illumination for a solar cell with an active layer spin-coated from a chlorobenzene solution (SC), a solar cell with an inkjet-printed active layer from a chloro-/trichlorobenzene ink that was dried at 130 °C (IP1) and a solar cell with inkjet-printed passive and active layers (IP2). Both of the passive layers for SC and IP1 were spin-coated from PEDOT:PSS.

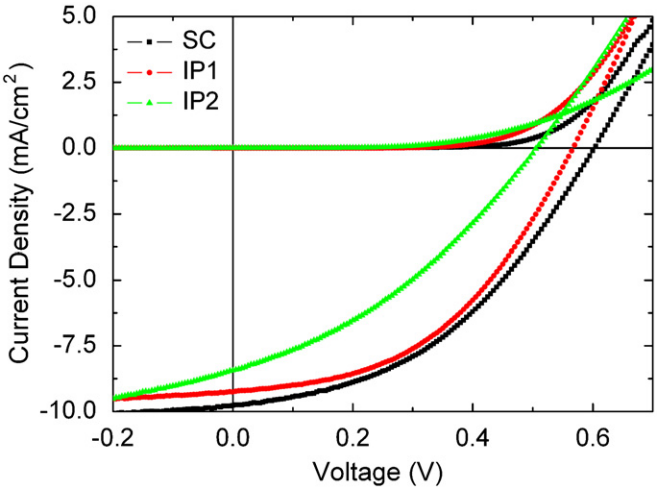

Fig. 3. Current density versus voltage for solar cells SC (spin-coated passive and active layers), IP1 (spin-coated passive layer and inkjet-printed active layer) and IP2 (inkjet-printed passive and active layers).

Table 1
Summary of the performance of solar cells SC, IP1 and IP2 shown in Fig. 3 showing the open circuit voltage V_{oc}, the short circuit current J_{sc}, the fill factor *FF* and the η_{PCE}.

Device Type	V_{oc} (V)	J_{sc} (mA/cm^2)	*FF* (%)	η_{PCE} (%)
SC	0.603	9.69	45	2.64
IP1	0.573	9.34	45	2.40
IP2	0.507	8.94	34	1.54

Fig. 3 shows that the performance of the IP1 solar cell is similar to that of the SC solar cell. A small difference is seen in the V_{oc} but this is attributed to possible thickness variations in the inkjet-printed film. This result indicates that the chloro/trichlorobenzene inkjet solvent system can be used to generate solar cells with comparable performance to those of spin-coated devices that were prepared according to traditional procedures. However, spin-coated and inkjet-printed active layers had different thicknesses, 110 versus 180 nm, respectively. It is possible that the efficiency of a device with a thicker spin-coated active layer would be greater then 2.64% due to a higher degree of light absorption resulting in a higher short circuit current density [23]. Table 1 shows a performance summary for the solar cells shown in Fig. 3.

In order to examine the inkjet-printed and spin-coated films in more detail, the surface topographies of these films were analyzed with atomic force microscopy (AFM). During spin-coating, a solid film can be generated within seconds upon rotation. This does not occur during inkjet-printing, where the film is in a fluid state for a longer period of time. Due to these differences, variations in the surface topographies of spin-coated and inkjet-printed films are possible. Fig. 4 shows AFM images of spin-coated and inkjet-printed films.

Despite the different preparation procedures for spin-coated and inkjet-printed films, the surface topographies are surprisingly similar as shown in Fig. 4. The root mean square roughness (R_{rms}) for the spin-coated and printed films was found to be ~1.4 nm in both cases. The R_{rms} values compare well with approximately 3 nm reported for other spin-coated pre-annealed P3HT:PCBM films [24]. Slight differences between the two types of films are indicated by the peak to valley heights of 11.7 and 19.1 nm for the spin-coated and inkjet-printed films, respectively. This indicates

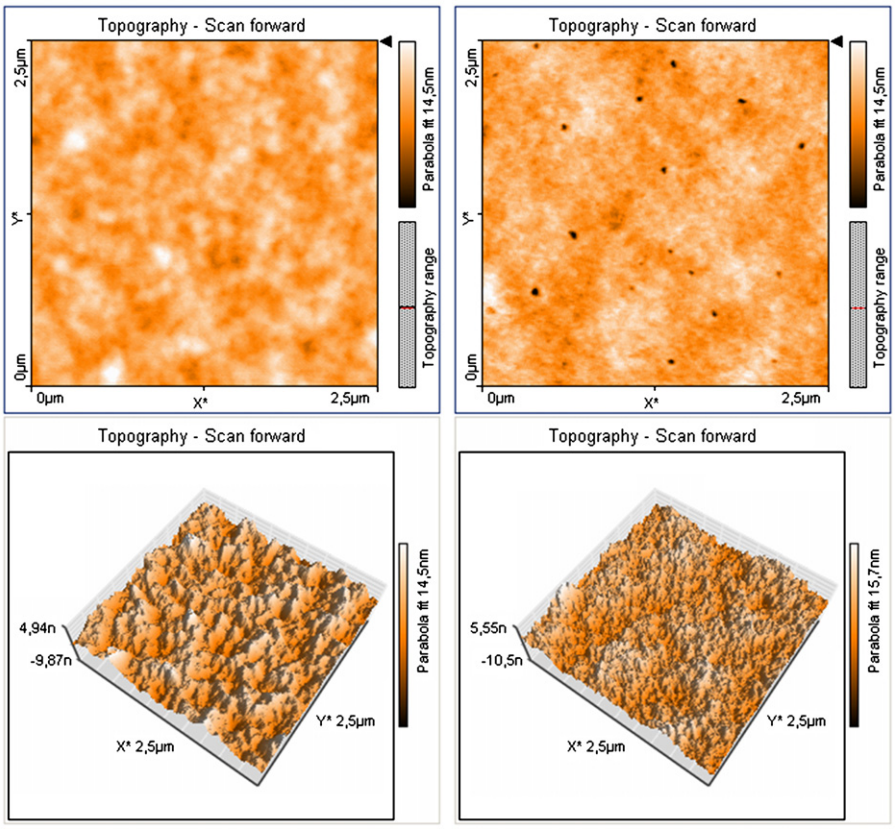

Fig. 4. AFM images of spin-coated (left) and inkjet-printed (right) P3HT:PCBM films measured after pre-annealing.

that with the given ink formulation and thermal treatments, drying at 130 °C and pre-annealing at 100 °C for 30 min, the surface roughness of the inkjet-printed and spin-coated films is similar. Analysis of the surface topography of post-annealed P3HT:PCBM films has not yet been successfully performed due to the difficulty in removing the cathode without damaging the polymer layers. It has been reported that hydrochloric acid can be used to dissolve the aluminium cathode of P3HT:PCBM solar cells [24]. This method was used and it was unsuccessful because all of the solar cell layers were removed. In conclusion, the chloro-/trichlorobenzene inkjet solvent mixture was used to generate printed solar cells with similar performance to spin-coated solar cells. This could be attributed to an optimum length of phase separation in the printed films, which is similar to that of a spin-coated film as shown in Fig. 4.

Given the potential of inkjet-printing to be used for multiple thin film processing steps, a solar cell was generated where both the passive and active layers were inkjet-printed (IP2). This device demonstrated a η_{PCE} of 1.5%, which compares with η_{PCE} of 2.4% when only the active layer of a solar cell was printed (IP1). This is currently the highest reported performance of a solar cell with inkjet-printed passive and active layers to our knowledge. Despite the lower performance of IP2, solar cells can be produced where traditional technologies such as spin-coating are replaced by inkjet-printing.

The reduced performance of IP2 as indicated in Table 1 can be due to the series resistance. A higher series resistance for IP2 is supported by lower dark current densities at positive voltages when compared with SC and IP1. The series resistance acts to lower the current at a given voltage and reduce the fill factor in organic solar cells [25]. Probable cause of the increased series resistance in IP2 is the addition of isopropanol and ethylene glycol to the passive layer ink used for inkjet-printing. It has been reported that conductivity of inkjet-printed PEDOT:PSS films changes by two orders of magnitude when 6 wt% glycerol was added to the respective ink [26]. The addition of the solvents to the passive layer ink used for this report could have changed the packing of the polymer particles in the film. In order to further quantify the series resistance of the three types of solar cells, inverse slope of the current density–voltage plot above V_{oc} under illumination was found. For solar cells SC and IP1, the series resistance after post-annealing was calculated as 18 and 15 cm^2, which compares with 24–35 cm^2 for IP2. This indicates that the series resistance is slightly higher for the solar cell with printed passive and active layers.

In addition to the series resistance, thickness of the printed layers could also be the origin of the reduced performance of IP2. Printed passive layers had thicknesses of 110 versus 30 nm for spin-coated PEDOT:PSS layers. A large printed passive layer thickness was needed to generate a homogeneous and complete film. Because of this, the sum of the passive and active layer thicknesses of IP2 was 290 nm, where 140 nm was found for SC and 210 nm for IP1. Thicker printed layers would increase the series resistance because charges in the film would need to travel greater distances to reach the electrodes. As the distance to the electrodes increases, the chances of a charge becoming trapped or recombining also increases.

4. Conclusions

In this work, solar cells with P3HT:PCBM inkjet-printed active layers were reported to reach η_{PCE} of 2.4% when the solvent system consisted of chlorobenzene and trichlorobenzene. Relatively good solubility of P3HT in trichlorobenzene resulted in printed films with optimal phase separation when compared with spin-coated films as indicated by AFM. In addition, the importance of drying conditions after printing was demonstrated where an optimal drying temperature of 130 °C was found. Usefulness of the P3HT:PCBM ink consisting of chloro- and trichlorobenzene was further shown when it was inkjet-printed onto printed passive layers, which generated solar cells with a η_{PCE} of 1.5%. Future work will focus on optimizing the morphology of films printed from chloro- and trichlorobenzene. The ratio of the two solvents will be varied and the resulting influence on performance will be examined.

Acknowledgements

The authors would like to thank Dr. Frank Jaiser, University of Potsdam, for stimulating discussions. Funding was provided by the German Federal Ministry of Education and Research (BMBF), Project no. 13N10317.

References

[1] F.C. Krebs, Fabrication and processing of polymer solar cells: a review of printing and coating techniques, Sol. Energy Mater. Sol. Cells 93 (2009) 394–412.
[2] M. Helgesen, R. Søndergaard, F.C. Krebs, Advanced materials and processes for polymer solar cell devices, J. Mater. Chem. 20 (2010) 36–60.
[3] G. Dennler, M.C. Scharber, C.J. Brabec, Polymer–fullerene bulk-heterojunction solar cells, Adv. Mater. 21 (2009) 1323–1338.
[4] F.C. Krebs, K. Norrman, Using light-induced thermocleavage in a roll-to-roll process for polymer solar cells, ACS Appl. Mater. Interfaces 2 (2010) 877–887.
[5] F.C. Krebs, S.A. Gevorgyan, J. Alstrup, A roll-to-roll process to flexible polymer solar cells: model studies, manufacture and operational stability studies, J. Mater. Chem. 19 (2009) 5442–5451.
[6] F.C. Krebs, S.A. Gevorgyan, B. Gholamkhass, S. Holdcroft, C. Schlenker, M.E. Thompson, B.C. Thompson, D. Olson, D.S. Ginley, S.E. Shaheen, H.N. Alshareef, J.W. Murphy, W.J. Youngblood, N.C. Heston, J.R. Reynolds, S. Jia, D. Laird, S.M. Tuladhar, J.G.A. Dane, P. Atienzar, J. Nelson, J.M. Kroon, M.M. Wienk, R.A.J. Janssen, K. Tvingstedt, F. Zhang, M. Andersson, O. Inganäs, M. Lira-Cantu, R. de Bettignies, S. Guillerez, T. Aernouts, D. Cheyns, L. Lutsen, B. Zimmermann, U. Würfel, M. Niggemann, H.F. Schleiermacher, P. Liska, M. Grätzel, P. Lianos, E.A. Katz, W. Lohwasser, B. Jannon, A round robin study of flexible large-area roll-to-roll processed polymer solar cell modules, Sol. Energy Mater. Sol. Cells 93 (2009) 1968–1977.
[7] F.C. Krebs, T.D. Nielsen, J. Fyenbo, M. Wadstrøm, M.S. Pedersen, Manufacture, integration and demonstration of polymer solar cells in a lamp for the Lighting Africa initiative, Energy Environ. Sci. 3 (2010) 512–525.
[8] L.M. Chen, Z. Hong, G. Li, Y. Yang, Recent progress in polymer solar cells: manipulation of polymer:fullerene morphology and the formation of efficient inverted polymer solar cells, Adv. Mater. 21 (2009) 1434–1449.
[9] W. Ma, C. Yang, X. Gong, K. Lee, A.J. Heeger, Thermally stable efficient polymer solar cells with nanoscale control of the interpenetrating network morphology, Adv. Funct. Mater. 15 (2005) 1617–1622.
[10] S.H. Park, A. Roy, S. Beupre, S. Cho, N. Coates, J.S. Moon, D. Moses, M. Leclerc, K. Lee, A.J. Heeger, Bulk heterojunction solar cells with internal quantum efficiency approaching 100%, Nat. Photon. 3 (2009) 297–302.
[11] M. Al-Ibrahim, O. Ambacher, S. Senfuss, G. Gobsch, Effects of solvent and annealing on the improved performance of solar cells based on poly (3-hexylthiophene): fullerene, Appl. Phys. Lett. 86 (2005) 201120 201120-1–201120-3.
[12] R.D. Deegan, Pattern formation in drying drops, Phys. Rev. E 61 (2000) 475–485.
[13] B.J. de Gans, U.S. Schubert, Inkjet printing of well-defined polymer dots and arrays, Langmuir 20 (2004) 7789–7793.
[14] C.N. Hoth, S.A. Choulis, P. Schilinsky, C.J. Brabec, High photovoltaic performance of inkjet printed polymer:fullerene blends, Adv. Mater. 19 (2007) 3973–3978.
[15] C.N. Hoth, P. Schilinsky, S.A. Choulis, C.J. Brabec, Printing highly efficient organic solar cells, Nano Lett. 8 (2008) 2806–2813.
[16] C.N. Hoth, S.A. Choulis, P. Schilinsky, C.J. Brabec, On the effect of poly (3-hexylthiophene) regioregularity on inkjet printed organic solar cells, J. Mater. Chem. 19 (2009) 5398–5404.
[17] T. Aernouts, T. Aleksandrov, C. Girotto, J. Genoe, J. Poortmans, Polymer based organic solar cells using ink-jet printed active layers, Appl. Phys. Lett. 92 (2008) 033306 033306-1–033306-3.
[18] United States Environmental Protection Agency 1,2,4-trichlorobenzene fact sheet, November 2004, 〈http://epa.gov/chemfact/tcben-sd.pdf〉.
[19] W.Y. Huang, C.C. Lee, T.L. Hsieh, The role of conformational transitions on the performance of poly(3-hexylthiophene)/Fullerene solar cells, Sol. Energy Mater. Sol. Cells 93 (2009) 382–386.
[20] M. Koppe, C.J. Brabec, S. Heiml, A. Schausberger, W. Duffy, M. Heeney, I. McCulloch, Influence of molecular weight distribution on the gelation of

P3HT and its impact on the photovoltaic performance, Macromolecules 42 (2009) 4661–4666.
[21] G. Li, Y. Yao, H. Yang, V. Shrotriya, G. Yang, Y. Yang, Solvent Annealing effect in polymer solar cells based on poly(3-hexylthiophene) and methanofullerenes, Adv. Funct. Mater. 17 (2007) 1636–1644.
[22] J. Ouyang, Y. Xia, High-performance polymer photovoltaic cells with thick P3HT:PCBM films prepared by a quick drying process, Sol. Energy Mater. Sol. Cells 93 (2009) 1592–1597.
[23] H. Jin, J. Olkkonen, M. Tuomikoski, P. Kopola, A. Maaninen, J. Hast, Thickness dependence and solution-degradation effect in poly(3-hexylthiophene): phenyl-C61-butyric acid methyl ester based solar cells, Sol. Energy Mater. Sol. Cells 94 (2010) 465–470.
[24] H. Kim, W.W. So, S.J. Moon, The importance of post-annealing process in the device performance of poly(3-hexylthiophene): methanofullerene polymer solar cell, Sol. Energy Mater. Sol. Cells 91 (2006) 581–587.
[25] S.S. Sun, N.S. Sariciftci, in: Organic Photovoltaics, CRC Press, Boca Raton, FL, 2005, p. 276.
[26] S.H. Eom, S. Senthilarasu, P. Uthirakumar, S.C. Yoon, J. Lim, C. Lee, H.S. Lim, S.H. Lee, Polymer solar cells based on inkjet-printed PEDOT:PSS layer, Org. Electron. 10 (2009) 536–542.